

The Turing Pattern Transition with the Growing Domain and Metabolic Rate Effects

Shin Nishihara ^{1*} and Toru Ohira ¹

¹ Graduate School of Mathematics, Nagoya University.

Furocho, Chikusaku, Nagoya, 464-8602, Japan.

*Corresponding author: shin.kurokawa.c8@math.nagoya-u.ac.jp

Abstract

The present study investigates the phenomenon of pattern transitions on the body surfaces of mammals during their transition from juveniles to adults and with seasonal changes. Our previous research suggests that patterns formed during infancy may disperse due to the growing domain (GD) effects, but their transition is sensitive to parameter values. Thus, in the present study, we focus on a factor that can change due to domain growth, such as heat. Generally, the greater the ratio of surface area to volume, the more easily heat within it is dissipated. Hence, it can be considered that smaller organisms may lose heat more easily while larger organisms may retain it more effectively. In fact, thermoregulation during infancy is a crucial factor directly influencing survival.

We propose a theoretical model, incorporating GD and Metabolic-Rate (MR) effects, to elucidate the underlying mechanisms robustly driving these pattern transitions. The model suggests that Turing patterns formed during juvenile stages disperse in adulthood, due to domain growth and changes in metabolic rates affecting reaction rates. Numerical analysis results demonstrate that when both the GD and the MR effects are incorporated, patterns disperse more rapidly compared to the case where only the GD effects are considered.

Additionally, we discuss the potential correlations among pattern transitions, growth, and thermoregulation mechanisms, highlighting the importance of metabolic rates in maintaining temperature within the domain. Our findings provide insights into the complex interplay between growth, thermoregulation, and pattern transitions in mammals, possibly useful for further research in this field.

Keywords: domain growth, metabolic rate, endothermic thermoregulation, pattern formation, pattern transition

1. Introduction

If the appearance of parents and children were significantly different, there might be significance in elucidating the causes and purposes of these differences: there might be new discoveries or insights awaiting exploration. For instance, in the case of the Chinese softshell turtle (*Pelodiscus sinensis*), the patterns on the plastron formed during the embryonic/juvenile stages disappear as the turtle grows, to the extent that comparing only the plastron might make them appear as entirely different creatures. It has been suggested that this phenomenon of pattern transition may theoretically be explained by the Growing-Domain effects, where the domain of the plastron grows [Nishihara and Ohira, 2024]. However, unlike the case of pattern transition in the less visually prominent ventral side of the reptile, many mammals exhibit clearly identifiable and readily distinguishable patterns that undergo transition. For example, in species such as wild boars (*Sus scrofa*), lions (*Panthera leo*), sika deer (*Cervus nippon*), and tapirs (*Tapirus indicus* and *terrestris*), the patterns on their body surfaces are distinctly different between juveniles and adults. In contrast to the non-Turing patterns on the plastron of *P. sinensis*, Turing patterns such as spots and/or stripes are observed on the body surface of these juveniles, which disappear as they mature. In the case of adult sika deer, a cycle exists in which the same patterns as those of their juvenile are formed during the summer and disappear during the winter. In Malayan tapirs, slightly different from the South American tapirs, although the patterns from their juvenile stages vanish in adulthood, the body surface in the adult tapirs is clearly divided into white and black domains. Despite such subtle differences between species, the phenomenon of patterns formed on the body surface during the juvenile stages disappearing in adulthood is consistently observed in these mammals.

The present study aims to explore the possibility that patterns are formed as a "byproduct" based on some survival strategies of theirs, because if the patterns on the body surfaces of these mammalian juveniles serve a role in camouflage to escape from their predators, then the patterns of lion cubs, for example, may not need to persist into adulthood as their roles undoubtedly transition from prey to predator, whereas, for tapirs, there may be no need to deliberately eliminate the camouflage patterns formed during their calf stages as they remain prey even as adults (in the first place, regarding the visibility of prey to predators, it is only possible to speculate [Filip Jaroš, 2012]). By conceptualizing the patterns formed during the juvenile stages as Turing patterns and considering the theoretical elements that may lead to the dispersion of these Turing patterns, this study suggests exploring their survival strategies that may imply the formation and dispersion of patterns as "byproducts."

Similar to the theoretical proposal for the pattern transition on the plastron of the Chinese softshell turtle [Nishihara and Ohira, 2024], it is proposed that the Growing-Domain effects may contribute to the pattern transition in these mammals due to the clear growth of the domain. However, it was also mentioned that there were cases where patterns do not disperse despite the effects [Nishihara and Ohira, 2024], indicating the possibility of other mechanisms inducing pattern transition. In particular, focusing on the fact that thermogenesis is crucial to the survival of mammalian newborns [Bienboire-Frosini et al., 2023], the differences in thermoregulation due to the domain differences between juveniles and adults may also induce changes in metabolic rates, resulting in the efficient thermogenesis for newborns and the dispersion of Turing patterns on their body surface in adulthood. Regarding endothermic thermogenesis in mammals, thermoregulations through brown adipose tissue (BAT) and muscle nonshivering thermogenesis have been studied [Berg et al., 2006; Bienboire-Frosini, et al., 2023; Gaudry et al., 2017a; Gaudry et al., 2017b; Nowack et al., 2019; Ricquier, 2005] and in particular, for instance, the mechanism of thermoregulation in wild boars changes over time as they mature [Bienboire-Frosini et al., 2023]. The theoretical elements of the aforementioned Growing-Domain effects, in conjunction with changes in metabolic rates for their thermogenesis induced by domain differences, may synergistically function to induce pattern transitions on the body surfaces between these mammalian juveniles and adults.

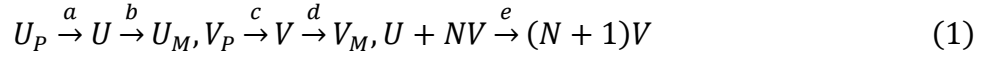
The present study proposes that the Turing pattern transition on the body surfaces of mammals can be theoretically induced by the Growing-Domain ('GD') and/or Metabolic-Rate ('MR') effects associated with the domain growth.

2. Modeling of Turing Pattern Transition Induced by GD and/or MR Effects

The previous study [Nishihara and Ohira, 2024] modeled the phenomenon where the black patterns on the plastron of *P. sinensis* are formed during the embryonic and juvenile stages and gradually disappear in the adult stage, based on the GD effects in the reaction-diffusion system. However, it is not pattern formation induced by Turing Instability, and those black patterns cannot be considered as Turing patterns. Hence, in this study, we propose a model for the phenomenon where Turing patterns formed based on Turing instability can undergo transition. For example, lions (*Panthera leo*) and wild boars (*Sus scrofa*) exhibit patterns resembling Turing patterns, such as spots and stripes, during their juvenile stage, which disappear as they mature (specific differences in pattern colors can be interpreted based on the assumption of whether morphogen acts as an activator or inhibitor [Bard, 1981]).

Furthermore, even in sika deer (*Cervus nippon*), the spotted patterns on their body surface transition between summer and winter, even in the absence of the domain-growth condition (*i.e.*, the phenomenon of the pattern forming and dispersing is repeated in the fixed domain). In other words, it is suggested that the model we should explore includes additional effects besides the GD effects.

Thus, we first analyze the influence of the GD effects on Turing patterns caused by Turing instability, illustrating specific reaction terms (however, it should be noted that these reaction terms are not mandatory but merely one example). The following reactions for certain substances U and V (U_P , for example, refers to the precursor of the substance U , while U_M refers to, for instance, a metabolite of U . The same applies to V_P and V_M) with $N \in \mathbb{N}$:



introduces the reaction terms below:

$$\begin{aligned} F(U, V) &:= -eUV^N + a - bU, G(U, V) := eUV^N + c - dV, \\ U[M], V[M], a \left[\frac{M}{\text{sec}} \right], b \left[\frac{1}{\text{sec}} \right], c \left[\frac{M}{\text{sec}} \right], d \left[\frac{1}{\text{sec}} \right], e \left[\frac{1}{M^N \cdot \text{sec}} \right]. \end{aligned} \quad (2)$$

With the reaction terms under the condition $N = 2$ (see Appendix-A for other values of N) and diffusion coefficients (ϕ_u and ϕ_v [cm^2/sec]), a reaction-diffusion system on a spatially fixed domain is described as:

$$\begin{aligned} \frac{\partial U}{\partial t} &= \phi_u \left(\frac{\partial^2}{\partial X^2} + \alpha_u \frac{\partial^2}{\partial Y^2} \right) U + F(U, V), \\ \frac{\partial V}{\partial t} &= \phi_v \left(\frac{\partial^2}{\partial X^2} + \alpha_v \frac{\partial^2}{\partial Y^2} \right) V + G(U, V), \end{aligned} \quad (3)$$

where α_u, α_v are constants that represent anisotropy (*i.e.*, $\alpha_u, \alpha_v = 1$ means isotropy), with the zero-flux boundary conditions applied. Furthermore, in order to facilitate the analysis of key points in the model, we partially nondimensionalize the system as follows:

$$\begin{aligned} \frac{\partial u}{\partial t} &= \phi_u \nabla_u^2 u + f(u, v), \text{ where } f(u, v) := \mu(-uv^2 - \beta u + \beta), \\ \frac{\partial v}{\partial t} &= \phi_v \nabla_v^2 v + g(u, v), \text{ where } g(u, v) := \mu(uv^2 - \delta v + \varepsilon), \\ u &:= \frac{b}{a} U, v := \frac{b}{a} V, \mu := \frac{a^2 e}{b^2}, \beta := \frac{b^3}{a^2 e}, \delta := \frac{b^2 d}{a^2 e}, \varepsilon := \frac{b^3 c}{a^3 e}, \end{aligned} \quad (4)$$

where μ has the dimension $[1/\text{sec}]$, and $\nabla^2 := \partial^2/\partial X^2 + \alpha \cdot \partial^2/\partial Y^2$. When μ equals 1, the

conditions for Turing Instability capable of forming Turing patterns are described as:

$$\begin{aligned} f_u^* + g_v^* < 0, \quad f_u^* g_v^* - f_v^* g_u^* > 0, \\ \phi_v f_u^* + \phi_u g_v^* > 0, \quad (\phi_v f_u^* + \phi_u g_v^*)^2 - 4\phi_u \phi_v (f_u^* g_v^* - f_v^* g_u^*) > 0, \end{aligned} \quad (5)$$

where $f_u = -v^2 - \beta$, $f_v = -2uv$, $g_u = v^2$, $g_v = 2uv - \delta$, while f_u^* , for instance, is defined as $\partial f / \partial u$ at the equilibrium point (u^*, v^*) and the others are defined similarly (see Appendix-A for details). Hence, based on Turing Instability, the discrete wavenumbers (k^2) that can form Turing patterns should exist in the following range of values k_-^2 and k_+^2 [Murray, 2013]:

$$k_{\pm}^2 := \frac{1}{2\phi_u \phi_v} \left(\phi_v f_u^* + \phi_u g_v^* \pm \sqrt{(\phi_v f_u^* + \phi_u g_v^*)^2 - 4\phi_u \phi_v (f_u^* g_v^* - f_v^* g_u^*)} \right). \quad (6)$$

Moreover, even when $\mu \neq 1$, the conditions described above are essentially unchanged, while the discrete wavenumbers' range is changed and described as μk_{\pm}^2 . Based on the definitions of μ, β, δ , and ε , it is technically possible to increase or decrease only μ in the system (4). Increasing μ leads to an increase in wavenumber and a decrease in wavelength, while decreasing μ results in a decrease in wavenumber and an increase in wavelength. In other words, in this model, μ can be considered as the controller for adjusting the wavelength of Turing patterns, as mentioned in other studies [Murray, 2013; Woolley et al., 2021]. For instance, it is suggested that if you want to create large spotted patterns, you should set a small μ , whereas if you want to form small spotted patterns, then you should set a large μ . In this paper, μ can be understood as metabolic rates from the equations (1) and (4), where larger/smaller μ may suggest higher/lower metabolic rates.

We have discussed Turing Instability in a domain that does not grow with time, so far. However; actual organisms and tissues grow with time, so we construct a model by applying a domain that grows with time, the GD effects, to the model mentioned above. With the growing domain applied to the system (4), the model with the GD effects is described as:

$$\begin{aligned} \frac{\partial u}{\partial t} &= \frac{\phi_u}{r^2(t)} \left(\frac{\partial^2}{\partial x^2} + \alpha_u \frac{\partial^2}{\partial y^2} \right) u + f(u, v) - \frac{2r'(t)}{r(t)} u, \\ \frac{\partial v}{\partial t} &= \frac{\phi_v}{r^2(t)} \left(\frac{\partial^2}{\partial x^2} + \alpha_v \frac{\partial^2}{\partial y^2} \right) v + g(u, v) - \frac{2r'(t)}{r(t)} v, \end{aligned} \quad (7)$$

where $(X, Y) := (r(t)x, r(t)y)$, $r(t)$ is a length-scaling function, and $r'(t) := dr/dt$ [Nishihara and Ohira, 2024]. In order to simplify discussions, let $r(t)$ be defined as $\exp(d_a t/2)$, where d_a is a positive constant, to ensure that the dilution terms do not become time-dependent (this is merely an example for the sake of discussion simplification), and then it is assumed that the domain growth based on $r(t)$ starts from a certain time point t_g . Hence, during growing stages ($t \geq t_g$) the system (7) is specifically described as:

$$\begin{aligned}\frac{\partial u}{\partial t} &= \frac{\phi_u}{\exp(d_a(t - t_g))} \left(\frac{\partial^2}{\partial x^2} + \alpha_u \frac{\partial^2}{\partial y^2} \right) u + \mu \left(-uv^2 - \left(\beta + \frac{d_a}{\mu} \right) u + \beta \right), \\ \frac{\partial v}{\partial t} &= \frac{\phi_v}{\exp(d_a(t - t_g))} \left(\frac{\partial^2}{\partial x^2} + \alpha_v \frac{\partial^2}{\partial y^2} \right) v + \mu \left(uv^2 - \left(\delta + \frac{d_a}{\mu} \right) v + \varepsilon \right).\end{aligned}\quad (8)$$

Thus, if d_a is selected such that the conditions for Turing Instability are met at $t = t_g$, then even as time progresses, those conditions will continue to be approximately satisfied as far as the linear theory allows. Additionally, the system (8) suggests that, as time elapses, larger wavenumbers (corresponding to smaller wavelengths) which can form Turing patterns start to be included in the range of μk_{\pm}^2 . This case suggests the possibility that the Turing pattern formed until then ($t < t_g$) does not disappear. Since the phenomenon discussed in this paper is the dispersion of formed patterns, we use and analyze d_a from this point onwards, which no longer satisfies Turing Instability at $t = t_g$, suggesting the potential dispersion of Turing patterns.

However, the seasonal pattern transition on the body surface of sika deer is unlikely to be explained only by the GD effects. Furthermore, concerning the pattern transition in lions and wild boars, it would require unrealistic time frames for the patterns to disappear, potentially necessitating the unrealistic growth of the animals into giant adults. Therefore, we focus on the possibility of small μ inducing Turing patterns with very large wavelengths that could lead to pattern dispersion. Based on the principle of surface area-to-volume ratios, considering that juveniles may critically require more metabolic heat than adults [Bienboire-Frosini et al., 2023], the present study proposes that if it is assumed that the domain growth can decrease μ , it would likely be when μ has a positive correlation with metabolic rates. Thus, in order to incorporate another equation for the temperature T [°C] correlated with μ into system (8) following Pennes' Bioheat Equation, we consider the case where $Q(T)$ [W/m²], the metabolic rate, is adjusted such that $T = T_{th}$, which is a certain constant, and since the perfusion term correlates with the metabolic rate, for convenience, it is defined herein as included within the logistic-type function, $Q(T)$, in this paper [Marn et al., 2019; Shrestha et al., 2020; Singh, 2024] (this study focuses on a two-dimensional domain [Othmer et al., 2009]), with the Dirichlet boundary condition applied: $T|_{\partial\Omega} = 0$. For example, the following equation including the perfusion term (*i.e.*, $\rho_b c_b w_b (T_{th} - T)$ in the equation (10) below) will be a possible consideration:

$$\rho c \frac{\partial T}{\partial t} = \rho c \phi_{\tau} \nabla^2 T + \kappa \rho c T_{th} \cdot T \left(1 - \frac{T}{T_{th}} \right), \quad (9)$$

where $\rho[kg/m^2]$, $c[J/(kg \cdot ^\circ C)]$, $\phi_\tau[m^2/sec]$, $\kappa[1/(^\circ C \cdot sec)]$ are positive constants, and $\nabla^2 := \partial^2/\partial X^2 + \alpha_\tau \partial^2/\partial Y^2 [1/m^2]$, and although the same spatial variables are employed in this paper for the sake of simplification of discussions, it is important to recognize that such a constraint does not exist. Note that both the perfusion term and the metabolic rate term can be defined as indicated by the following equations, and then both terms are included in $Q(T)$ to express it as shown in the equation (9):

$$Q(T) = \kappa \rho c T_{th} T \left(1 - \frac{T}{T_{th}}\right) := \rho_b c_b w_b (T_{th} - T) + \kappa \rho c T'_{th} \cdot T' \left(1 - \frac{T'}{T'_{th}}\right), \quad (10)$$

where $T' := T - (\rho_b c_b w_b / \kappa \rho c)$. Defining $\tau := T/\lambda$ using a positive constant $\lambda[^\circ C]$ to nondimensionalize T leads to the following equation:

$$\frac{\partial \tau}{\partial t} = \phi_\tau \nabla^2 \tau + q(\tau), \quad (11)$$

where $q(\tau) := \kappa \lambda \tau (\tau_{th} - \tau) [1/sec]$, and $\tau_{th} := T_{th}/\lambda$, with $\tau|_{\partial\Omega} = 0$, and we define the average $q(\tau)$, the metabolic rate, per unit area in the domain at each t as $\bar{q}(\tau)$, and define $\hat{\mu}(\tau)$ for metabolic rate effects at the time as $\hat{\mu}(\tau) := \gamma \bar{q}(\tau)$ where γ is a positive constant as $\hat{\mu}(\tau)$ has a positive correlation with metabolic rates in the present study. The metabolic rate, $q(\tau)$, is defined under the assumption that metabolic heat is generated at all points, in the equation (11). Although there is no necessity to calculate the area-average value of $q(\tau)$, the metabolic heat generation on the boundary becomes relatively higher compared to the interior of the domain since the equation (11) imposes the Dirichlet boundary conditions. This heterogeneity on the domain becomes a somewhat intricate point for discussing pattern transitions, hence we use $\bar{q}(\tau)$ in this paper. Therefore, to explain the pattern transition on the body surfaces of the mammals mentioned earlier, the present study proposes the following model by incorporating the GD and MR effects:

$$\begin{aligned} \frac{\partial u}{\partial t} &= \frac{\phi_u}{r^2(t)} \left(\frac{\partial^2}{\partial x^2} + \alpha_u \frac{\partial^2}{\partial y^2} \right) u + \hat{\mu}(\tau) (-uv^2 + \beta(1-u)) - \frac{2r'(t)}{r(t)} u, \\ \frac{\partial v}{\partial t} &= \frac{\phi_v}{r^2(t)} \left(\frac{\partial^2}{\partial x^2} + \alpha_v \frac{\partial^2}{\partial y^2} \right) v + \hat{\mu}(\tau) (uv^2 - \delta v + \varepsilon) - \frac{2r'(t)}{r(t)} v, \\ \frac{\partial \tau}{\partial t} &= \frac{\phi_\tau}{r^2(t)} \left(\frac{\partial^2}{\partial x^2} + \alpha_\tau \frac{\partial^2}{\partial y^2} \right) \tau + q(\tau) - \frac{2r'(t)}{r(t)} \tau, \\ \hat{\mu}(\tau) &:= \gamma \bar{q}(\tau), \text{ where } \bar{q}(\tau) := \frac{\int_{\Omega} q(\tau) dS}{|\Omega|} \text{ at each } t, \end{aligned} \quad (12)$$

with the zero-flux boundary conditions applied for u, v , and $\tau|_{\partial\Omega} = 0$.

3. Result

We compare numerically how Turing patterns (spots) formed in the system (4) without the GD or MR effects transition in the systems (7) and (8) with only the GD effects, and in the system (12) with both GD and MR effects. As shown in the numerical analysis results below, even in the systems (7) and (8) with only the GD effects, the patterns disperse, but in the system (12) with both the GD and MR effects, the patterns disperse more quickly. In the former case, the patterns disperse when the domain grows by approximately 16.4 times, whereas in the latter case, the patterns disperse with a growth of 7.4 times, where in the former case the patterns are still being formed (see the cross-sectional view for details).

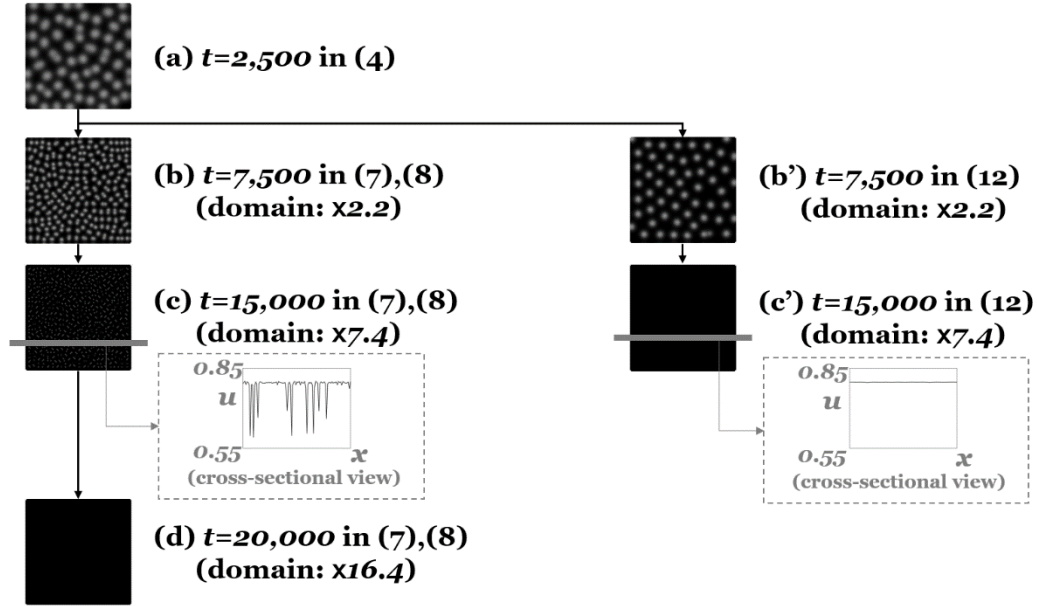


Figure 1. The numerical analysis results: (a) the pattern formed at $t = t_g = 2,500$ in the system (4), (b)(c)(d) those at $t = 7,500$, $15,000$, and $20,000$ in the systems (7) and (8), respectively, (b')(c') those at $t = 7,500$, and $15,000$ in the system (12), under the parameters: $(\phi_u, \phi_v, \beta, \delta, \varepsilon, d_a, \mu(\text{the initial value in the system (4)}), \alpha_u, \alpha_v, \phi_\tau, \alpha_\tau, \kappa\lambda, \tau_{th}, \gamma) = (0.21, 0.05, 0.07, 0.18, 0.01, 3.2 \times 10^{-4}, 0.5, 1.0, 1.0, 0.24, 1.0, 0.2, 0.5, 300)$.

In addition, even in cases of slower growth (for instance, when $d_a = 2.0 \times 10^{-4}$), although requiring more time ($t = 23,000$) the patterns similarly disappear in the system (12), whereas in the systems (7) and (8), they are still formed at the same time point (see Appendix-B).

As mentioned earlier, in the case of sika deer, their spotted patterns transition with seasonal changes without the growth of the domain. In other words, the pattern transition on sika deer's body surface may follow the system (13) described below, which removes the GD effect from the system (12). Note that the system (13) differs from the system (12) in that

while the system (12) achieves pattern transitions without altering the coefficient values, the system (13) requires intentional modification of the coefficient $\kappa\lambda$, as will be discussed later. This necessity to intentionally change the value of coefficient $\kappa\lambda$ distinguishes the numerical analysis results obtained from the system (12) and those from the system (13).

$$\begin{aligned}\frac{\partial u}{\partial t} &= \phi_u \left(\frac{\partial^2}{\partial x^2} + \alpha_u \frac{\partial^2}{\partial y^2} \right) u + \hat{\mu}(\tau)(-uv^2 + \beta(1-u)), \\ \frac{\partial v}{\partial t} &= \phi_v \left(\frac{\partial^2}{\partial x^2} + \alpha_v \frac{\partial^2}{\partial y^2} \right) v + \hat{\mu}(\tau)(uv^2 - \delta v + \varepsilon), \\ \frac{\partial \tau}{\partial t} &= \phi_\tau \left(\frac{\partial^2}{\partial x^2} + \alpha_\tau \frac{\partial^2}{\partial y^2} \right) \tau + q(\tau).\end{aligned}\tag{13}$$

In this case, the MR effects (changes) are not induced as there is no GD effect. Hence, assuming that the efficiency of metabolic heat generation in sika deer decreases in the winter, decreasing the coefficient, $\kappa\lambda$, in $q(\tau)$ resulted in numerical analysis results showing the dispersion of the spotted patterns as follows.

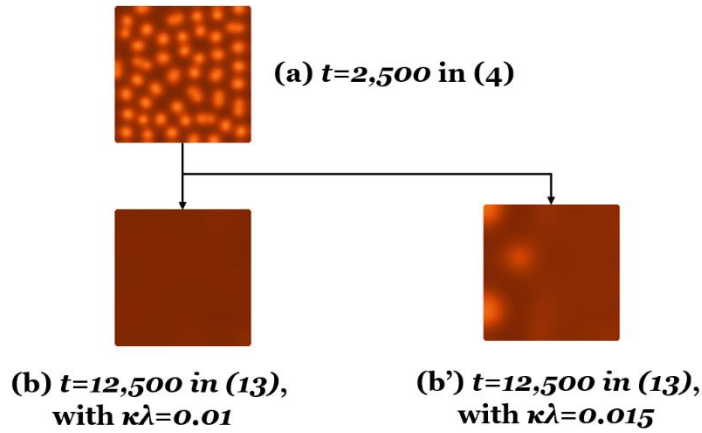


Figure 2. The numerical analysis results: (a) the pattern formed at $t = t_g = 2,500$ in the system (4) under the same parameters as those of Fig. 1a, (b)(b') those at $t = 12,500$ in the system (13) with $\kappa\lambda = 0.01$, and 0.015 , respectively. (Figures in Color)

4. Conclusion

In mammals, there are species that alter the patterns on their body surfaces during the process of transitioning from juveniles to adults, as well as with seasonal changes. In this paper, we theoretically and abstractly conceptualize this phenomenon, proposing a model in which Turing patterns initially formed transition due to the growth of the domain and the associated changes in metabolic rates. While the present study has demonstrated that Turing patterns can disperse due to the GD effects (dilution and diffusion coefficient

decrease) as shown in the previous study [Nishihara and Ohira, 2024], comparing these results with actual phenomena has revealed unrealistic aspects (for example, requiring growth to a giant domain for pattern dispersion). Therefore, we focus on the possibility that metabolic rates relatively decrease within the grown domain to be able to efficiently maintain temperature within the domain due to growth, and propose a model incorporating the MR effects (decrease in metabolic rates). As a result, the dispersion of the patterns has been confirmed in domains of realistic sizes more quickly than in cases with only the GD effect, due to the combined action of both the GD and MR effects. Furthermore, by applying only the MR effect for cases where the domain does not grow, *i.e.*, patterns transition with seasonal changes without the GD effect, pattern dispersion has been reproduced by modifying the coefficient associated with the MR effect. In conclusion, the present study theoretically proposes that Turing patterns formed based on a certain chemical reaction disperse and/or transition due to the growth of the domain (the GD effect) and changes in metabolic rates affecting reaction rates (the MR effect).

5. Discussion

First and foremost, it should be emphasized that the model proposed in this paper, the system (12), is not derived from solid experiments but rather is a theoretically proposed model that abstractly captures the transition of patterns on the body surfaces of mammals. It is undoubtedly agreeable that mammals undergo significant growth from juveniles to adults, and temperature is crucial for them. The former is self-evident, and regarding the latter, especially for newborns, thermoregulation is literally a matter of life and death [Bienboire-Frosini et al., 2023], and resolving this issue for survival is inevitable. For instance, in the case of wild boars, it has been confirmed that patterns transition during the growth process from juveniles to adults and that the mechanisms of thermoregulation change [Bienboire-Frosini et al., 2023]. While it is premature to directly link these two aspects, it cannot be denied that there may be some correlation, which would be a topic for future research. For example, in cold environments, prioritizing metabolic heat generation over adenosine triphosphate (ATP) production for thermoregulation may lead to the upregulation of AgRP mRNA only when ATP levels are low, resulting in the inhibition of α -MSH specifically under such conditions, which could induce pattern transition in response to environmental/seasonal changes [Plotkin et al., 2022; Shimizu et al., 2008] (it should be noted that it has not been demonstrated in wild boars). Additionally, lions are suggested to have different thermoregulation mechanisms from wild boars, such as using BAT/UCP1, similar to the Siberian tigers (*Panthera tigris altaica*) and leopards (*Panthera pardus*)

which belong to the same genus [Berg et al., 2006; Gaudry et al., 2017b]. Lions are imagined to inhabit environments where they can escape from extremely cold conditions upon reaching adulthood, whereas, however; the Siberian tigers need to continue living in extremely cold environments even as adults, and maintaining metabolic heat is essential for survival [Carroll and Miquelle, 2006]. Interestingly, the Siberian tigers maintain the same patterns on their body surfaces as when they were juveniles. On the other hand, the habitat of leopards differs from that of lions and Siberian tigers, being vast [Zeng et al., 2022]. Hence, survival strategies akin to those of the Siberian tiger in extreme cold environments might have been prioritized, possibly leading to the lack of pattern transitions from juveniles to adults on leopards' body surface, but it should be noted that they maintain the same patterns as juveniles even as adults, highlighting the fact that pattern transitions cannot be explained solely by thermoregulation mechanisms and habitat.

On the other hand, in the case of sika deer, pattern transitions are synchronized with habitat changes: metabolism increases in summer and decreases in winter. Under the assumption that the metabolic rates increase/decrease during summer/winter, the system (13) reproduces this pattern transition. Especially in winter, there are individuals where spots remain on the body surface to some extent, and it is worth considering that this difference is reproduced by the slight difference in metabolic rates, $\kappa\lambda$.

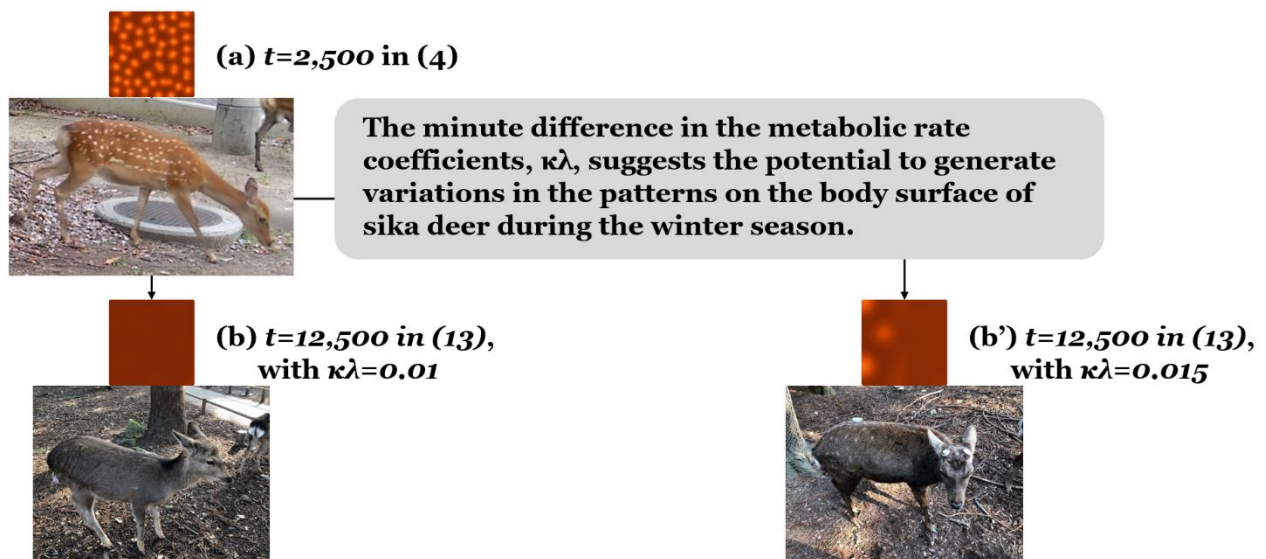


Figure 3. The same results of the numerical analysis as those of Fig. 2, with the actual photograph of deer (in September, 2023 (the upper one) and February, 2024 (the bottom ones)). (Figures and Photos in Color)

Moreover, it has been confirmed that elk (*Cervus elaphus nelson*) have lower metabolic rates

in specific environments [Parker et al., 1984]. There may be a similar mechanism in sika deer. And this survival strategy of decreasing metabolic rates may correspond to the possibility that the total number of respiratory cycles throughout life remains constant [Escala et al., 2022]. However, it should be noted again that this is not a conclusively proven conclusion.

In an exceptional case differing from the spotted patterns, when changing α_v , the coefficient representing the anisotropy in the horizontal direction (y -axis direction in this case) of Fig. 1, from 1.0 to 0.7 (it is assumed to diffuse from the dorsal line [Bard, 1981]), the striped patterns formed in the system (4) disperse at $t = 17,000$ (when the domain has grown to approximately 10.2 times its original size) both in the systems (7) and (8) (in cases not involving the MR effect) and in the system (12) (see Appendix-C). As suggested by the exceptional case, it should be noted that patterns may not necessarily disperse more quickly due to the combined actions of the GD and MR effects (as the value of α_v decreases, it is confirmed by numerical analysis results that patterns are less likely to disperse (see Appendix-D)). Malayan tapirs, like American tapirs, have such striped patterns formed during their juvenile stage that transition as they grow into adults. However, unlike American tapirs, Malayan tapirs have distinct white and black areas that are clearly demarcated in all individuals, as one of notable exceptions [Othmer et al., 2009]. For example, as shown in Fig. 4, if only the value of ε in a certain domain (Ω_W in Fig. 4) changes during the growing-domain stages, meaning the production reaction rate of substance V varies based on the equations (1) and (4), a pattern resembling white and black domains will form. Similarly, the patterns on the surface of the calves are not uniformly stripes; rather, those of the head, forelimbs, and hindlimbs are spots. As mentioned in previous studies [Woolley et al., 2021], theoretically, simpler patterns should be formed on smaller domains such as the head and limbs compared to the torso. It might also be possible to induce spotted patterns in these domains, by employing spatial heterogeneity [Woolley et al., 2021], *i.e.*, by altering the value of α_v , for instance. However, the specific nature of substance V , as well as the reason for the variation in its production reaction rate and anisotropy, remains unclear and is within the realm of theoretical speculation.

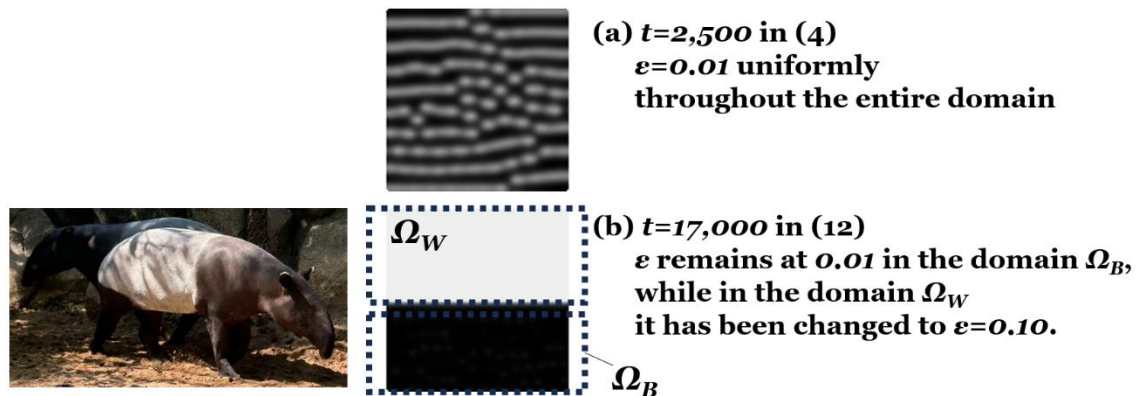


Figure 4. The numerical analysis results: (a) the pattern formed at $t = t_g = 2,500$ in the system (4) under the same parameters as those of Fig.1a, (b) the pattern formed at $t = 17,000$ in the system (12) with $\varepsilon|_{\Omega_W}$ changed from 0.01 to 0.10 ($\varepsilon|_{\Omega_B}$ unchanged). The figure of (a) resembles the pattern of the Malayan tapir's juvenile, while that of (b) resembles that of the adult (in January, 2024). (Photo in Color)

6. CRediT author statements

Shin Nishihara: Conceptualization, Methodology, Software, Validation, Formal analysis, Investigation, Resources, Data Curation, Writing - Original Draft, Writing - Review and Editing, and Visualization

Toru Ohira: Resources, Writing - Review and Editing, Supervision, Project administration, and Funding acquisition

7. Acknowledgements

This work was supported by JSPS Topic-Setting Program to Advance Cutting-Edge Humanities and Social Sciences Research Grant Number JPJS00122674991, and by Ohagi Hospital, Hashimoto, Wakayama, Japan.

8. References

J. B. L. Bard. A model for generating aspects of zebra and other mammalian coat patterns. *Journal of Theoretical Biology*, 93(2):363-385, 1981. doi: [https://doi.org/10.1016/0022-5193\(81\)90109-0](https://doi.org/10.1016/0022-5193(81)90109-0)

F. Berg et al. The Uncoupling Protein 1 Gene (UCP1) Is Disrupted in the Pig Lineage: A Genetic Explanation for Poor Thermoregulation in Piglets. *PLOS GENETICS*, 2006. doi:

<https://doi.org/10.1371/journal.pgen.0020129>

C. Bienboire-Frosini et al. The Role of Brown Adipose Tissue and Energy Metabolism in Mammalian Thermoregulation during the Perinatal Period. *Animals*, 13(13), 2023. doi: <https://doi.org/10.3390/ani13132173>

C. Carroll and D. E. Miquelle. Spatial viability analysis of Amur tiger *Panthera tigris altaica* in the Russian Far East: the role of protected areas and landscape matrix in population persistence. *Journal of Applied Ecology*, 43(6):1056-1068, 2006. doi: <https://doi.org/10.1111/j.1365-2664.2006.01237.x>

A. Escala. Universal relation for life-span energy consumption in living organisms: Insights for the origin of aging. *Scientific Reports*, 12:2407, 2022. doi: <https://doi.org/10.1038/s41598-022-06390-6>

M. J. Gaudry et al. Inactivation of thermogenic UCP1 as a historical contingency in multiple placental mammal clades. *SCIENCE ADVANCES*, 3(7), 2017a. doi: <https://doi.org/10.1126/sciadv.1602878>

M. J. Gaudry et al. Evolution of UCP1 Transcriptional Regulatory Elements Across the Mammalian Phylogeny. *Front. Physiol.*, 8, 2017b. doi: <https://doi.org/10.3389/fphys.2017.00670>

F. Jaroš. The ecological and ethological significance of felid coat patterns (Felidae). *Charles University in Prague*, Thesis. doi: <https://doi.org/10.13140/RG.2.2.25552.51209>

J. Marn et al. Relationship between metabolic rate and blood perfusion under Fanger thermal comfort conditions. *Journal of Thermal Biology*, 80:94-105, 2019. doi: <https://doi.org/10.1016/j.jtherbio.2019.01.002>

J. D. Murray. *Mathematical Biology II: Spatial Models and Biomedical Applications*. Springer, 2013.

S. Nishihara and T. Ohira. The mechanism of pattern transitions between formation and dispersion. *Journal of Theoretical Biology*, 581, 2024. doi: <https://doi.org/10.1016/j.jtbi.2024.111736>

J. Nowack et al. Muscle nonshivering thermogenesis in a feral mammal. *Scientific Reports*, 9(6378), 2019. doi: <https://doi.org/10.1038/s41598-019-42756-z>

H. G. Othmer et al. The Intersection of Theory and Application in Elucidating Pattern Formation in Developmental Biology. *Math. Model. Nat. Phenom.*, 4(4):3-82, 2009. doi: <https://doi.org/10.1051/mmnp/20094401>

K. L. Parker and C. T. Robbins. Thermoregulation in mule deer and elk. *Canadian Journal of Zoology*, 62(7), 1984. doi: <https://doi.org/10.1139/z84-202>

A. P. Plotkin. Appetite Control With Ageing: A Narrative Review Focused on the POMC and AgRP Neurons. *Reinvention*, 15:1, 2022. doi: <https://doi.org/10.31273/reinvention.v15i1.707>

D. Ricquier. Respiration uncoupling and metabolism in the control of energy expenditure. *Proceedings of the Nutrition Society*, 64(1):47-52, 2005. doi: <https://doi.org/10.1079/PNS2004408>

H. Shimizu et al. Glucocorticoids Increase Neuropeptide Y and Agouti-Related Peptide Gene Expression via Adenosine Monophosphate-Activated Protein Kinase Signaling in the Arcuate Nucleus of Rats. *Endocrinology*, 149(9):4544-4553, 2008. doi: <https://doi.org/10.1210/en.2008-0229>

D. C. Shrestha et al. Modeling on Metabolic Rate and Thermoregulation in Three Layered Human Skin during Carpentering, Swimming and Marathon. *Applied Mathematics*, 11(8), 2020. doi: <https://doi.org/10.4236/am.2020.118050>

M. Singh. Modified Pennes bioheat equation with heterogeneous blood perfusion: A newer perspective. *International Journal of Heat and Mass Transfer*, 218, 2024. doi: <https://doi.org/10.1016/j.ijheatmasstransfer.2023.124698>

T. E. Woolley et al. Bespoke Turing Systems. *Bulletin of Mathematical Biology*, 83(41), 2021. doi: <https://doi.org/10.1007/s11538-021-00870-y>

J. Zeng et al. Effects of Climate Change on the Habitat of the Leopard (*Panthera pardus*) in

the Liupanshan National Nature Reserve of China. *Animals*, 12(14), 2022. doi:
<https://doi.org/10.3390/ani12141866>

Appendix

A. The Conditions of Turing Instability in the System (4)

Since the equilibrium state (u^*, v^*) in the system (4) satisfies the equation described below:

$$u^* = \frac{\beta + \varepsilon - \delta v^*}{\beta}, \quad (A1)$$

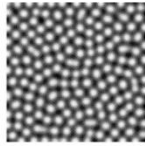
v^* is determined by the following equation based on the reaction terms in the system (4):

$$\delta v^3 - (\beta + \varepsilon)v^2 + \beta\delta v - \beta\varepsilon = 0. \quad (A2)$$

Expressing f_u^* , f_v^* , g_u^* and g_v^* in terms of v^* as shown below with $N \in \mathbb{N}$ ($N = 2$ in the system (4)):

$$f_u^* = \mu(-v^{*N} - \beta) < 0, \quad f_v^* = \mu(-Nu^*v^{*N-1}) = -N\mu\left(\delta - \frac{\varepsilon}{v^*}\right) < 0, \quad g_u^* = \mu v^{*N} > 0, \\ g_v^* = \mu(Nu^*v^{*N-1} - \delta) = \mu\left((N-1)\delta - \frac{N\varepsilon}{v^*}\right), \quad (A3)$$

$\phi_v f_u^* + \phi_u g_v^* > 0$ in the equation (5) requires $g_v^* > 0$, leading to the condition: $N \geq 2$. While the case of $N = 2$ is discussed in the main body of this paper, the cases of $N = 3, 4$, for example, in the system (4) also can form Turing patterns under the parameter spaces: $(\phi_u, \phi_v, \beta, \delta, \varepsilon) := (0.21, 0.05, 0.05, 0.12, 0.02)$ and $(0.21, 0.05, 0.03, 0.06, 0.01)$ for $N = 3$ and 4, respectively.



(a) $N=3$



(b) $N=4$

Figure A-1. The numerical analysis results: (a) the pattern formed at $t = 1,000$ in the system (4) under the parameters: $(\phi_u, \phi_v, \beta, \delta, \varepsilon, \mu, N) = (0.21, 0.05, 0.05, 0.12, 0.02, 1.0, 3)$, (b) that at $t = 1,000$ in the systems (4) under the parameters: $(\phi_u, \phi_v, \beta, \delta, \varepsilon, \mu, N) = (0.21, 0.05, 0.03, 0.06, 0.01, 1.0, 4)$

It should be noted that Turing Instability is never satisfied in the case of $N = 1$, so it is not taken into account in this paper.

B. Slower Growth and Pattern Transitions in the systems (4), (7), (8) and (12)

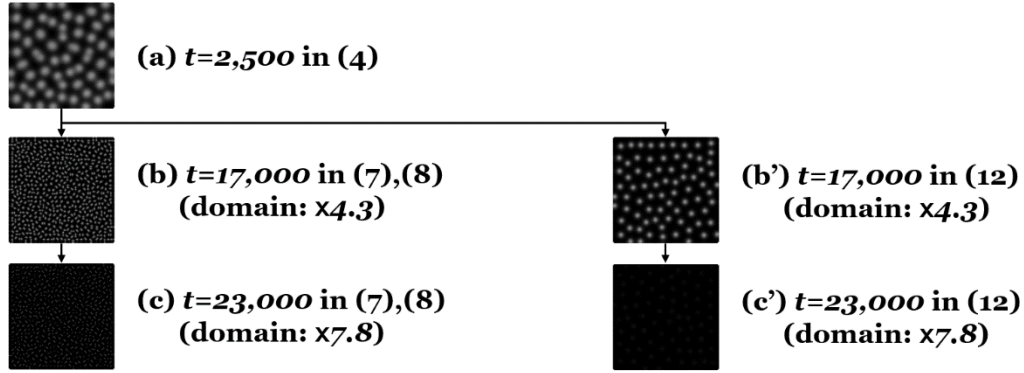


Figure B-1. The numerical analysis results: (a) the pattern formed at $t = t_g = 2,500$ in the system (4), (b)(c) those at $t = 17,000$, and $23,000$ in the systems (7) and (8), respectively, (b')(c') those at $t = 17,000$, and $23,000$ in the system (12), under the parameters:

$$(\phi_w, \phi_v, \beta, \delta, \varepsilon, d_a, \mu(\text{the initial value in the system (4)}), \alpha_w, \alpha_v, \phi_\tau, \alpha_\tau, \kappa\lambda, \tau_{th}, \gamma) = (0.21, 0.05, 0.07, 0.18, 0.01, 2.0 \times 10^{-4}, 0.5, 1.0, 1.0, 0.24, 1.0, 0.2, 0.5, 300).$$

C. Striped Pattern Transitions in the systems (4), (7), (8) and (12)

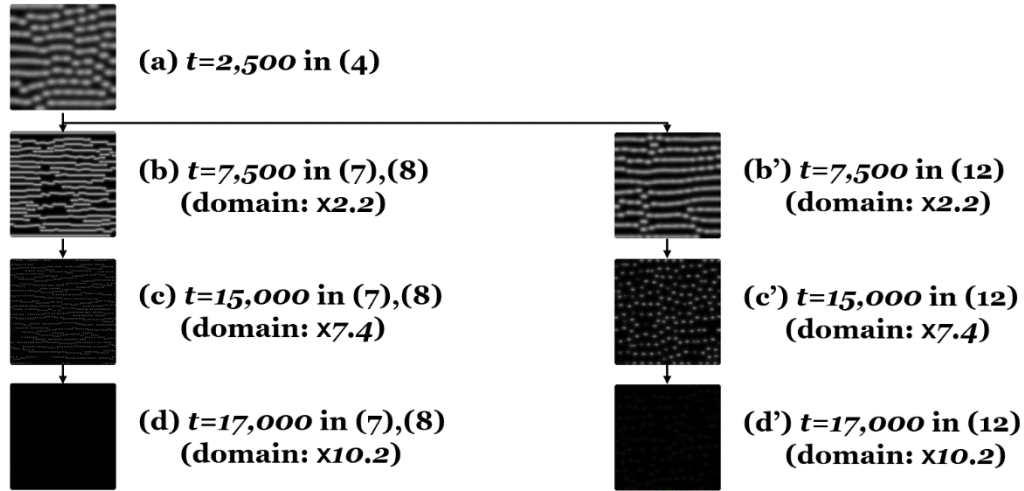


Figure C-1. The numerical analysis results: (a) the pattern formed at $t = t_g = 2,500$ in the system (4), (b)(c)(d) those at $t = 7,500$, $15,000$, and $17,000$ in the systems (7) and (8), respectively, (b')(c')(d') those at $t = 7,500$, $15,000$, and $17,000$ in the system (12), under the parameters:

$$(\phi_w, \phi_v, \beta, \delta, \varepsilon, d_a, \mu(\text{the initial value in the system (4)}), \alpha_w, \alpha_v, \phi_\tau, \alpha_\tau, \kappa\lambda, \tau_{th}, \gamma) = (0.21, 0.05, 0.07, 0.18, 0.01, 3.2 \times 10^{-4}, 0.5, 1.0, 0.7, 0.24, 1.0, 0.2, 0.5, 300).$$

D. The Relationship between Anisotropy and Pattern Dispersion

As the value of α_v indicating anisotropy decreases, there is an observed tendency for the

time (t) taken for patterns to disperse to increase, as demonstrated by the numerical analysis results below:

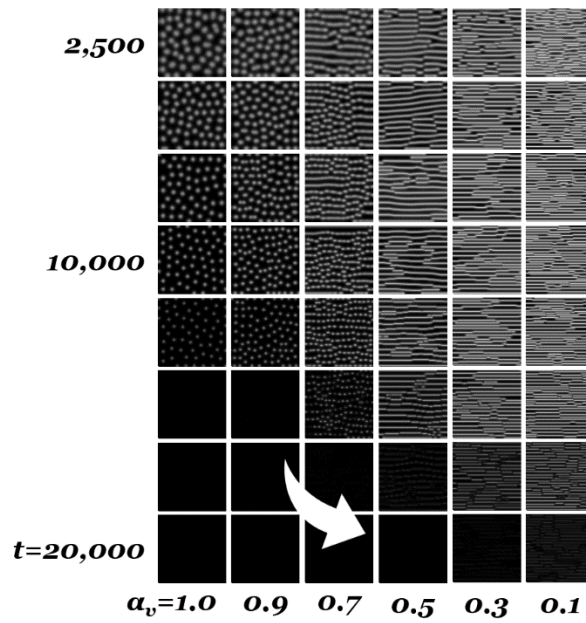


Figure D-1. The numerical analysis results: the patterns formed and dispersed at $t = 2,500, 5,000, 7,500, 10,000, 12,500, 15,000, 17,500,$ and $20,000$ in the system (12), under the parameters: $(\phi_w, \phi_v, \beta, \delta, \varepsilon, d_a, \mu(\text{the initial value in the system (4)}), \alpha_w, \phi_\tau, \alpha_\tau, \kappa\lambda, \tau_{th}, \gamma) = (0.21, 0.05, 0.07, 0.18, 0.01, 3.2 \times 10^{-4}, 0.5, 1.0, 0.24, 1.0, 0.2, 0.5, 300)$.